Physics Letters B 782 (2018) 646–651

Contents lists available at ScienceDirect

Physics Letters B

www.elsevier.com/locate/physletb

Differential cross section for $\gamma d \to \omega d$ using CLAS at Jefferson Lab

T. Chetry [a,*], K. Hicks [a,*], N. Compton [a], M. Sargsian [m], S. Adhikari [m], J. Ball [h], I. Balossino [r], L. Barion [r], M. Battaglieri [t], V. Batourine [aj,z], I. Bedlinskiy [x], A.S. Biselli [k,f], S. Boiarinov [aj], W.J. Briscoe [p], W.K. Brooks [ak,aj], V.D. Burkert [aj], D.S. Carman [aj], A. Celentano [t], G. Charles [ad], G. Ciullo [r,l], L. Clark [am], Brandon A. Clary [j], P.L. Cole [q], M. Contalbrigo [r], V. Crede [n], A. D'Angelo [u,af], N. Dashyan [aq], R. De Vita [t], E. De Sanctis [s], A. Deur [aj], C. Djalali [ah], R. Dupre [w], A. El Alaoui [ak], L. El Fassi [aa], P. Eugenio [n], G. Fedotov [a,ag], R. Fersch [i,ap], A. Filippi [v], G. Gavalian [aj,ab], Y. Ghandilyan [aq], K.L. Giovanetti [y], F.X. Girod [aj], E. Golovatch [ag], R.W. Gothe [ah], K.A. Griffioen [ap], L. Guo [m,aj], K. Hafidi [b], N. Harrison [aj], M. Hattawy [b], M. Holtrop [ab], Y. Ilieva [ah,p], D.G. Ireland [am], B.S. Ishkhanov [ag], E.L. Isupov [ag], D. Jenkins [an], S. Johnston [b], M.L. Kabir [aa], D. Keller [ao], G. Khachatryan [aq], M. Khachatryan [ad], M. Khandaker [ac], A. Kim [j], W. Kim [z], F.J. Klein [g], V. Kubarovsky [aj,ae], L. Lanza [u], P. Lenisa [r], K. Livingston [am], I.J.D. MacGregor [am], N. Markov [j], B. McKinnon [am], V. Mokeev [aj,ag], A. Movsisyan [r], C. Munoz Camacho [w], P. Nadel-Turonski [aj], S. Niccolai [w], G. Niculescu [y], M. Osipenko [t], A.I. Ostrovidov [n], M. Paolone [ai], R. Paremuzyan [ab], K. Park [aj,z], E. Pasyuk [aj,c], W. Phelps [m], O. Pogorelko [x], J.W. Price [d], Y. Prok [ad,ao], M. Ripani [t], D. Riser [j], B.G. Ritchie [c], A. Rizzo [u,af], G. Rosner [am], C. Salgado [ac], R.A. Schumacher [f], Iu. Skorodumina [ah], G.D. Smith [al], D.I. Sober [g], D. Sokhan [am], N. Sparveris [ai], S. Stepanyan [aj], I.I. Strakovsky [p], S. Strauch [ah,p], M. Taiuti [o], J.A. Tan [z], M. Ungaro [aj,ae], H. Voskanyan [aq], E. Voutier [w], L.B. Weinstein [ad], M.H. Wood [e,ah], N. Zachariou [al], J. Zhang [ao], Z.W. Zhao [ad]

[a] Ohio University, Athens, OH 45701, United States of America
[b] Argonne National Laboratory, Argonne, IL 60439, United States of America
[c] Arizona State University, Tempe, AZ 85287-1504, United States of America
[d] California State University, Dominguez Hills, Carson, CA 90747, United States of America
[e] Canisius College, Buffalo, NY, United States of America
[f] Carnegie Mellon University, Pittsburgh, PA 15213, United States of America
[g] Catholic University of America, Washington, D.C. 20064, United States of America
[h] IRFU, CEA, Universit'e Paris-Saclay, F-91191 Gif-sur-Yvette, France
[i] Christopher Newport University, Newport News, VA 23606, United States of America
[j] University of Connecticut, Storrs, CT 06269, United States of America
[k] Fairfield University, Fairfield CT 06824, United States of America
[l] Universita' di Ferrara, 44121 Ferrara, Italy
[m] Florida International University, Miami, FL 33199, United States of America
[n] Florida State University, Tallahassee, FL 32306, United States of America
[o] Università di Genova, 16146 Genova, Italy
[p] The George Washington University, Washington, DC 20052, United States of America
[q] Idaho State University, Pocatello, ID 83209, United States of America
[r] INFN, Sezione di Ferrara, 44100 Ferrara, Italy
[s] INFN, Laboratori Nazionali di Frascati, 00044 Frascati, Italy
[t] INFN, Sezione di Genova, 16146 Genova, Italy
[u] INFN, Sezione di Roma Tor Vergata, 00133 Rome, Italy
[v] INFN, Sezione di Torino, 10125 Torino, Italy
[w] Institut de Physique Nucléaire, CNRS/IN2P3 and Université Paris Sud, Orsay, France
[x] Institute of Theoretical and Experimental Physics, Moscow, 117259, Russia
[y] James Madison University, Harrisonburg, VA 22807, United States of America
[z] Kyungpook National University, Daegu 41566, Republic of Korea
[aa] Mississippi State University, Mississippi State, MS 39762-5167, United States of America
[ab] University of New Hampshire, Durham, NH 03824-3568, United States of America
[ac] Norfolk State University, Norfolk, VA 23504, United States of America
[ad] Old Dominion University, Norfolk, VA 23529, United States of America

https://doi.org/10.1016/j.physletb.2018.06.003

[ae] Rensselaer Polytechnic Institute, Troy, NY 12180-3590, United States of America
[af] Universita' di Roma Tor Vergata, 00133 Rome, Italy
[ag] Skobeltsyn Institute of Nuclear Physics, Lomonosov Moscow State University, 119234 Moscow, Russia
[ah] University of South Carolina, Columbia, SC 29208, United States of America
[ai] Temple University, Philadelphia, PA 19122, United States of America
[aj] Thomas Jefferson National Accelerator Facility, Newport News, VA 23606, United States of America
[ak] Universidad Técnica Federico Santa María, Casilla 110-V, Valparaíso, Chile
[al] Edinburgh University, Edinburgh EH9 3JZ, United Kingdom
[am] University of Glasgow, Glasgow G12 8QQ, United Kingdom
[an] Virginia Tech, Blacksburg, VA 24061-0435, United States of America
[ao] University of Virginia, Charlottesville, VA 22901, United States of America
[ap] College of William and Mary, Williamsburg, VA 23187-8795, United States of America
[aq] Yerevan Physics Institute, 375036 Yerevan, Armenia

ARTICLE INFO

Article history:
Received 19 February 2018
Received in revised form 23 April 2018
Accepted 3 June 2018
Available online 6 June 2018
Editor: V. Metag

Keywords:
Vector Meson Dominance
Differential cross section
Single scattering
Double scattering

ABSTRACT

The cross section for coherent ω-meson photoproduction off the deuteron has been measured for the first time as a function of the momentum transfer $t = (P_\gamma - P_\omega)^2$ and photon energy E_γ using the CLAS detector at the Thomas Jefferson National Accelerator Facility. The cross sections are measured in the energy range $1.4 < E_\gamma < 3.4$ GeV. A model based on $\omega - N$ rescattering is consistent with the data at low and intermediate momentum transfer, $|t|$. For $2.8 < E_\gamma < 3.4$ GeV, the total cross-section of $\omega - N$ scattering, based on fits within the framework of the Vector Meson Dominance model, is in the range of 30–40 mb.

1. Introduction

Vector meson photoproduction off protons at high energies is well described [1] theoretically using the phenomenological Vector Meson Dominance (VMD) model, in which the photon fluctuates into a virtual light vector meson (having the same quantum numbers as the photon) and then scatters off the target [2]. The VMD model has been very successful at predicting vector meson production at high energies. However, at photon energies closer to the production threshold, other diagrams, such as pseudoscalar meson exchange in the t-channel, can contribute [3]. This makes the reaction dynamics of vector meson photoproduction off proton targets more complex near threshold. Additional complexity near the threshold may come from nucleon resonances in the s-channel. Coherent ω-meson production off the deuteron avoids such complexities. Since both the deuteron and the final ωd state are isosinglets, exchange of non-isosinglet (e.g. pseudoscalar) mesons cannot contribute. Hence, natural parity exchange in the t-channel, usually described by Pomeron exchange (see Fig. 1a), is expected to dominate at low momentum transfer (low $|t|$, where $t = (P_\gamma - P_\omega)^2$ and P_i is the four-momentum of particle i) for vector meson photoproduction off deuterium, thus simplifying theoretical interpretations of the data.

At higher momentum transfer ($|t| > 0.5$ GeV$^2/c^2$) secondary scattering diagrams, where the ω is produced off one nucleon and scatters from the second, as shown in Fig. 1b, enable both nucleons to remain bound as a deuteron in the final state [4]. These diagrams provide an opportunity to extract the $\omega - N$ total scattering cross section, $\sigma_{\omega N}$, from comparisons of data and calculations. Similar studies were done for coherent ϕ-meson photoproduction from the deuteron [5,6], resulting in the first-ever estimates of the $\phi - N$ total cross section. Information on these vector meson–nucleon total cross sections is virtually impossible to extract cleanly via other methods, due to the short lifetimes of these mesons.

Experimental information on $\sigma_{\omega N}$ is of interest currently due to progress within lattice QCD, which can now extract meson–meson scattering phase shifts directly [7]. The Hadron Spectroscopy Collaboration [7] is working on extracting meson–nucleon scattering phase shifts, which are directly related to the total cross sections. This is a significant advance because it connects QCD calculations to experimental observables, such as the total cross sections. Such a direct connection between non-perturbative QCD and experiment has been rare until now. The ω meson is a particularly good choice for these studies, since it decays into three pions about 89% of the time. On the lattice, the light quark masses are inputs. Lattice results are often shown for pion masses heavier than in nature, as the lattice calculations are easier to compute there. The ω is thus a stable particle in lattice calculations where the pion mass is somewhat higher than its physical value. Scattering phase shifts of stable particles are easier to obtain on the lattice than for unstable particles. Hence, measurements of $\sigma_{\omega N}$ are timely and can soon be compared with predictions from lattice calculations.

Previous experimental data on coherent ω photoproduction are scarce. Bubble chamber measurements [1] have low statistical precision. The best data on this reaction are from the Weizmann Institute [8], using a photon beam of energy 4.3 GeV and at $|t| < 0.2$ GeV$^2/c^2$, which is too small to see the effect of double-scattering as shown in Fig. 1b. Data on coherent ρ photoproduction have been measured at higher $|t|$ at SLAC [9], which was used to extract $\sigma_{\rho N}$. No previous data exist that would allow an extraction of $\sigma_{\omega N}$.

Here, we present data on coherent ω photoproduction off deuterium at photon energies ranging from 1.4 to 3.4 GeV over a wide range in the momentum transfer t. The t-dependence of the cross section is measured out to $|t| \sim 2.0$ GeV$^2/c^2$, which is compared with theoretical calculations that include the double-scattering diagrams, allowing an extraction of the total scattering cross section $\sigma_{\omega N}$. This completes the measurement of scattering cross sections for the trio of vector mesons ($V = \rho, \omega, \phi$).

* Corresponding authors.
E-mail address: tc558111@ohio.edu (T. Chetry).

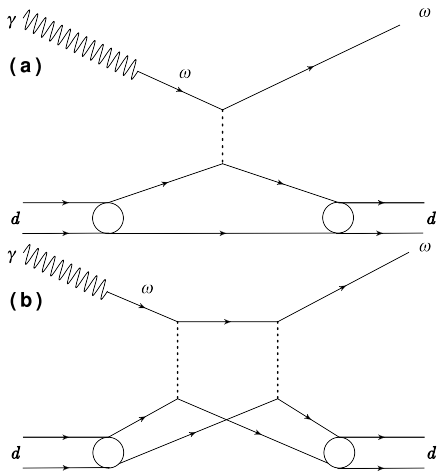

Fig. 1. t-Channel diagrams showing two ω-meson photoproduction mechanisms via **(a)** Single and **(b)** Double scattering. The photon fluctuates to the ω, which scatters off the nucleon(s). The dashed line represents the exchange of a Pomeron.

2. Experiment

The $g10$ dataset, with unpolarized beam, was collected in the spring of 2004 using the Continuous Electron Beam Accelerator Facility (CEBAF) and the CEBAF Large Acceptance Spectrometer (CLAS) at the Thomas Jefferson National Accelerator Facility (Jefferson Lab). CLAS was designed around six superconducting coils arranged in a toroidal configuration that produced a field in the azimuthal direction. The particle detection system consisted of six sets of drift chambers to determine charged-particle trajectories, gas Cherenkov counters to identify electrons, scintillator counters for measuring the time-of-flight (TOF) and electromagnetic calorimeters to detect neutrons and showering particles such as electrons. These segments were instrumented individually so that they formed actually independent magnetic spectrometers with a common target, trigger and data-acquisition system [10].

The $g10$ experiment used a continuous electron beam with incident electron energy, $E_e = 3.767$ GeV. This beam produced bremsstrahlung photons when passed through a thin gold radiator [10]. The tagger system [11] was used to measure the energy of the photons, which interacted with an unpolarized liquid deuterium target measuring 24 cm in length and 4 cm in diameter. The reaction products traversed the large drift chambers and timing detectors. The three-momenta were reconstructed by the drift chambers and the particle identification was determined by the arrival time of the products.

The data acquisition trigger required two charged particles detected in coincidence with the tagged photon. The time of flight of a particle was determined using the scintillator paddles in the start counter [12] that surrounded the target and the Time of Flight (ToF) scintillator paddles that surrounded the exterior of CLAS [13]. The charge of the particle was determined by its direction of bending in the magnetic field. We used the lower magnetic field (torus magnet current set at 2250 A) $g10$ dataset to optimize the acceptance for low-momentum in-bending π^- [14].

3. Data analysis

The exclusive reaction $\gamma d \to \omega d$ was identified by detecting a final-state deuteron and two charged pions from $\omega \to \pi^+\pi^-\pi^0$ decay. The unmeasured π^0 was reconstructed from the missing mass. Charged particles were identified from their measured three-momentum and measured flight time, using

$$\delta t = t_{measured} - \frac{d_{path}}{c}\frac{\sqrt{p^2+m^2}}{p}, \tag{1}$$

where d_{path} is the reconstructed path length of the particle from the event vertex to the ToF paddles, p is its momentum, and m is the assumed mass. The time difference for a charged particle about $\delta t = 0$ was fit as a function of the particle momentum with a Gaussian function for several momentum bins. A 3σ cut around the centroid of δt in each momentum bin was used to identify the particles in coincidence with a single photon.

The vertex time for each charged particle was compared to the arrival time for each photon (from the photon tagger). The photon with the time that most closely matched with the vertex time was selected. In order to remove multiple photons linked to one event, a timing cut of ± 1 ns was made. This cut helped to avoid ambiguity in selecting the "good" incident photon associated with an event of interest. The events rejected by this cut were studied separately and an overall correction, γ_{corr}, of 6.8% was found. γ_{corr} is the ratio of the number of rejected photons to the total number of photons associated with the final state detected particles for each event. The measured photon energy is slightly different from the real photon energy due to a slight geometrical mismatch, therefore photon energy correction (correction factor within 5%) explained in [15] was also applied to the energy of the selected photons.

With the identity of each scattered particle established, corrections were made for the energy lost by each detected charged particle while traveling through different materials of the detector [16]. In addition to the energy loss corrections for the charged particle tracks, slight corrections were also necessary for the momentum of each track, due to uncertainties in the magnetic field, by requiring four-momentum conservation using the exclusive $\gamma d \to \pi^+\pi^- d$ channel [17]. Cuts were also made to remove poorly performing ToF paddles. Events associated with beam trips were also removed from the analysis.

In addition to the above, fiducial region cuts were made to remove events that tracked back to non-physical regions of the detector or to regions of the detector where the efficiency was low or changing rapidly. Minimum momentum cuts were used to exclude particles with low detection efficiency. Events that tracked back to outside the target region were also removed [17].

The data analysis for $\gamma d \to \omega d$ consisted of two main steps: two-pion background rejection and ω yield extraction from the multi-meson background. The two-pion background is dominated by the $\gamma d \to \rho d$ channel as can be seen from Fig. 2a. The majority of this background was eliminated by requiring that the missing mass from the deuteron given by, $MM(\gamma d, d') = \sqrt{(P_d + P_\gamma - P_{d'})^2}$, equaled m_ω, assuming the three pion decay mode for the ω.

A missing π^0 peak can be seen on top of a smooth background in Fig. 2b, which was estimated by employing a Lorentzian for the peak and a second-order polynomial for the background. A 3σ cut, shown by the vertical dashed lines in Fig. 2b, was applied to select exclusive ω events with some background.

The missing mass spectra were then divided into four E_γ bins in $1.4 < E_\gamma < 3.4$ GeV, which were further split into different $|t|$ bins within $0.3 < -t < 2.0$ GeV$^2/c^2$. A total of 25 energy and momentum transfer bins were used to extract the number of ω-events. The ω-meson yield was obtained from a fit to the $MM(\gamma d, d')$ distribution by a Gaussian-convoluted Lorentzian function, also known as the Voigt profile, and a background function. The Lorentzian mean and width were fixed to 782.65 MeV/c^2 and 8.49 MeV/c^2 respectively, which correspond to the PDG mass and width of an ω-meson [18]. The Gaussian width, however, was allowed to vary. A polynomial function of second-order, $B(x) =$

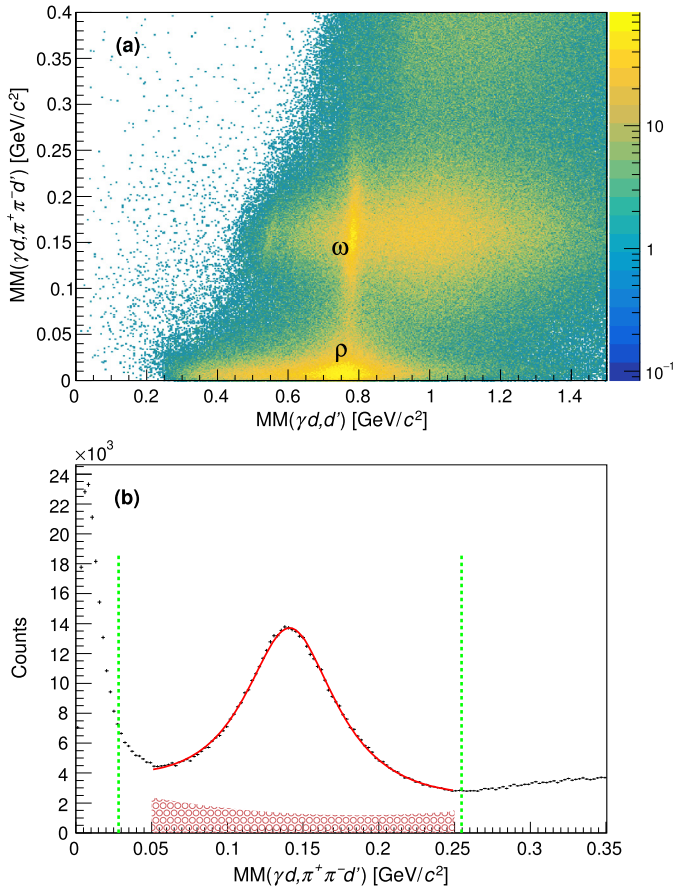

Fig. 2. **(a)** The y-axis represents the missing mass, Y, in the reaction $\gamma d \to \pi^+\pi^- d'\ Y$ while the x-axis shows the distribution of the missing mass, X, in the reaction $\gamma d \to d'\ X$. **(b)** Shown is the y-axis projection of (a). The vertical dashed lines represent the position of the missing mass cut made to select ω-events using the fit shown by the solid curve. An estimate of the possible background shape is shown by the shaded region.

$p_1 + p_2 x + p_3 x^2$ was chosen to estimate the multi-pion background, where $x \equiv MM(\gamma d, d)$, and the p_i are fit parameters. The yield was determined by integrating the Voigtian function. A linear function was used to estimate the systematic effect of the choice of the background function. An average systematic effect of about 8.6% was found due to the uncertainty of the background subtraction. The fit for one typical bin is shown in Fig. 3.

Measurement of the differential cross-section required a calculation of the CLAS acceptance based upon the geometrical efficiencies of the detector subsystems. The CLAS acceptance was determined by performing a GEANT-based Monte-Carlo simulation. As the acceptance is reaction dependent, $\gamma d \to \omega d \to \pi^+\pi^- d'(\pi^0)$ events were generated. These events underwent the same event processing as the data. For each kinematic bin, the acceptance was calculated as the ratio of the number of accepted to the generated events. The simulated distributions were also fit similar to the data. The average acceptance for this channel was found to be 8.1%.

The target luminosity was calculated from the incident photon flux (N_γ) for the collimated photon beam, target density (ρ_T), atomic weight ($M_d = 2.014$ g/mol) and length of the target (l_T) using the relation,

$$\mathscr{L}(E_\gamma) = \frac{\rho_T N_A l_T}{M_d} N_\gamma(E_\gamma), \tag{2}$$

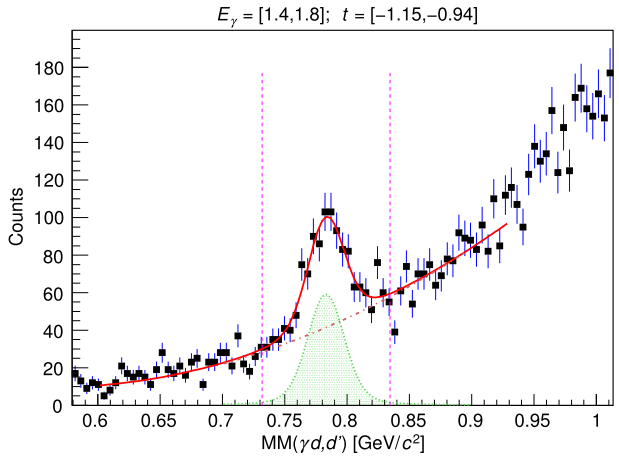

Fig. 3. Yield extraction fit using the missing mass distribution for $E_\gamma = 1.4$–1.8 GeV and $|t| = 0.94$–1.15 GeV$^2/c^2$. The background is estimated using a polynomial function (dashed-dotted) which, along with the signal (dashed, shaded region), describe the total distribution (solid curve). The yield is the number of events in the shaded region within the vertical dashed lines.

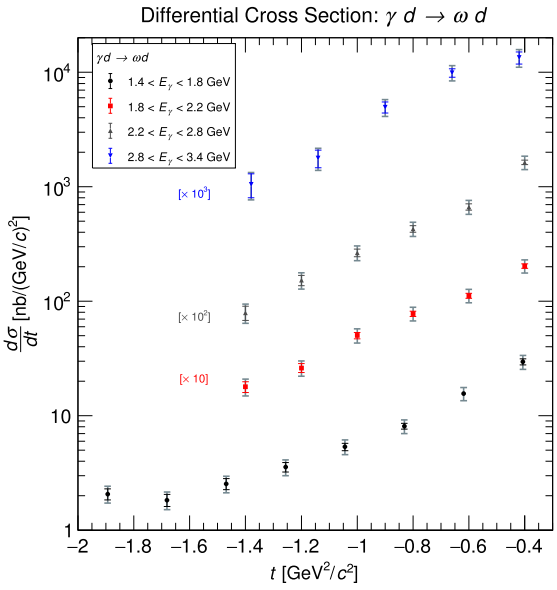

Fig. 4. Differential cross section for $\gamma d \to \omega d$. The inner error bars represent the statistical uncertainties while the outer error bars include systematic uncertainties added in quadrature with the statistical uncertainties.

where N_A is Avogadro's number. In each energy bin, the differential cross sections in momentum transfer bins of width Δt are calculated using the relation,

$$\frac{d\sigma}{dt} = \frac{Y_D}{\Delta t A \mathscr{L}} \times \frac{\Gamma_\omega}{\Gamma_{\omega\to\pi^+\pi^-\pi^0}} \times \gamma_{corr} \tag{3}$$

where Y_D is the yield, A is the detector acceptance, $\mathscr{L}$ is the target luminosity for the photon energy range considered and, $\Gamma_{\omega\to\pi^+\pi^-\pi^0}/\Gamma_\omega$ is the branching ratio. The quantity γ_{corr} is the correction factor due to the photon selection condition mentioned previously. The statistical uncertainty on the differential cross section was propagated from the uncertainties of each quantity in Eq. (3). The differential cross section for $\gamma d \to \omega d$ is shown in Fig. 4 as a function of $|t|$ for each incident photon energy bin.

Systematic uncertainties were determined for each part of the analysis including the effects of event selection, yield extraction, beam normalization, and so on. Table 1 summarizes the system-

Table 1
Summary of the g10 systematic effects associated with the $\gamma d \to \omega d$ channel, estimating a total average point-to-point uncertainty.

Source	Systematic uncertainty
Luminosity/Flux Consistency	8%
Variation of Cuts/Analysis	4.4%
Yield Extraction	8.6%
Branching Ratio	0.7%
Total (Added in quadrature)	12.5%

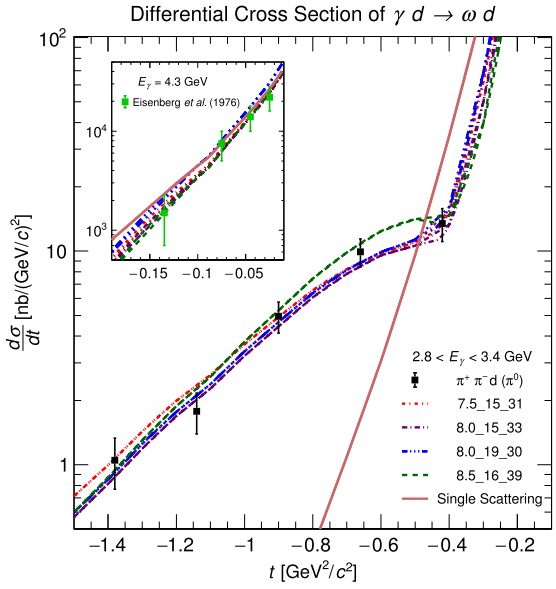

Fig. 5. Differential cross section of $\gamma d \to \omega d$ as a function of $|t|$ for $2.8 < E_\gamma < 3.4$ GeV compared to that of a calculation [21] based on [4]. Each curve corresponds to a specific b, $\frac{d\sigma}{dt}|_{t=0,\gamma N}$ and $\sigma_{\omega N}$ value, as listed in Table 2. The legend for each curve is defined respectively for these parameters. The solid curve represents the contribution of the single scattering for input parameters corresponding to that of the dashed-dotted curve. In the inset, the solid points are the results from [8] for an incident photon energy of 4.3 GeV.

atic uncertainties calculated in this experiment. Due to the large variation of the statistical uncertainty involved in this analysis, a point-to-point systematic approach was not realistic. Therefore, an estimation of the systematic errors was made by varying each cut and taking the average relative difference in the final result for each variation. These variations are summarized as different groups in Table 1.

4. Results

In Fig. 5, the differential cross section for $2.8 < E_\gamma < 3.4$ GeV is compared with a theoretical calculation using a rescattering model [4]. This is a three-parameter model allowing us to determine a range of $\sigma_{\omega N}$ by a fit to the experimental data. The scattering amplitude of $\gamma N \to \omega N$ given by

$$f^{\gamma N \to \omega N} = \sigma_{\gamma^* \omega}(i + \alpha_{\gamma N}) e^{\frac{-b_{\gamma N}}{2} t}, \quad (4)$$

deals with single scattering. A similar equation can be also written for the scattering amplitude of $\omega N \to \omega N$ that measures the contribution of the rescattering [4]. The quantity $\sigma_{\gamma^* \omega}$ is parametrized using an input parameter $\frac{d\sigma}{dt}|_{t=0,\gamma N}$, which is the differential cross section of $\gamma N \to \omega N$ reaction at $t = 0$. The initial guess for this parameter was based on published data on $\gamma p \to \omega p$ [19,20]. The

Table 2
Summary of theory parameters used to compare data for $2.8 < E_\gamma < 3.4$ GeV. The parameters shown here are within 15% of $\chi^2 = 1.0$ (the ideal value).

$b_{\gamma N} = b_{\omega N}$ [GeV$^{-2}/c^{-2}$]	$\frac{d\sigma}{dt}|_{t=0,\gamma N}$ [$\mu b/($GeV$^2/c^2)$]	$\sigma_{\omega N}$ [mb]	χ^2/NDF
7.5	15	31	1.13
8.0	14	34	1.15
8.0	15	33	1.01
8.0	16	32	0.96
8.0	17	31	1.00
8.0	18	30	1.15
8.0	19	30	0.91
8.0	19	31	0.87
8.0	20	30	1.03
8.5	16	35	1.11
8.5	16	39	1.00
8.5	17	34	1.05
8.5	18	33	1.07
9.0	19	39	0.89
9.0	20	38	0.87

other two input parameters are $b_{\gamma N}$ or $b_{\omega N}$ and $\sigma_{\omega N}$. At intermediate and higher photon energies, VMD assumes the slope factors of the corresponding amplitudes, $b_{\gamma N}$ and $b_{\omega N}$, to be equal. The variables, $\alpha_{\gamma N}$ and $\alpha_{\omega N}$, defined as the ratio of the real to imaginary parts of the corresponding scattering amplitudes, were kept fixed and equal to a phenomenological value of -0.4. At intermediate energies, the real part of the scattering amplitudes for proton and neutron targets are not exactly the same, but this model omits this difference since ω production from d is dominated by isospin averaged amplitudes [4]. Now, for various slope factors, the strength of single scattering gauged by $\frac{d\sigma}{dt}|_{t=0,\gamma N}$ is varied. Each set of variations was fed to the calculation for various $\sigma_{\omega N}$ values as an input parameter and the differential cross section values for a particular energy (bin center) were calculated. The outputs were compared with the data using a χ^2 test. Table 2 summarizes the values of these parameters that resulted in a reduced χ^2 between 0.85 and 1.15. The data is consistent with the rescattering model with $30 < \sigma_{\omega N} < 40$ mb in the framework of the VMD model.

5. Conclusion

In conclusion, we have presented the first measurement of the differential cross sections for coherent ω photoproduction on the deuteron up to $t = -2$ GeV$^2/c^2$ for incident photon energies 1.4 to 3.4 GeV using CLAS at Jefferson Lab. A model based on rescattering is consistent with the data at intermediate and high momentum transfer. The differential cross section at large $|t|$ shows contributions from double scattering. For $2.8 < E_\gamma < 3.4$ GeV, the data is consistent with $\sigma_{\omega N}$ within 30–40 mb. This range is typical of hadronic cross sections in this energy range. While more data would be valuable, this dataset dramatically improves the world data on the $\gamma d \to \omega d$ reaction and opens up the possibility for further study of the $\omega - N$ interaction.

Acknowledgements

We are grateful to the staff of the Accelerator and Physics Division at Jefferson Lab that made this experiment possible and helped us get results of better quality. This work was supported by: the United Kingdom's Science and Technology Facilities Council (STFC); the Chilean Comisiòn Nacional de Investigaciòn Cientìfica y Tecnològica (CONICYT); the Italian Istituto Nazionale di Fisica Nu-

cleare; the French Centre National de la Recherche Scientifique; the French Commissariat àl'Energie Atomique; the U.S. National Science Foundation; and the National Research Foundation of Korea. Jefferson Science Associates, LLC, operates the Thomas Jefferson National Accelerator Facility for the U.S. Department of Energy under Contract No. DE-AC05-06OR23177.

References

[1] T.H. Bauer, R.D. Spital, D.R. Yennie, F.M. Pipkin, The hadronic properties of the photon in high-energy interactions, Rev. Mod. Phys. 50 (1978) 261–436, https://doi.org/10.1103/RevModPhys.50.261.

[2] J. Sakurai, Theory of strong interactions, Ann. Phys. 11 (1) (1960) 1–48, https://doi.org/10.1016/0003-4916(60)90126-3.

[3] Y. Oh, A.I. Titov, T.S.H. Lee, Electromagnetic production of vector mesons at low-energies, in: Excited Nucleons and Hadronic Structure. Proceedings, Conference, NSTAR 2000, Newport News, USA, February 16–19, 2000, 2000, pp. 255–262, arXiv:nucl-th/0004055, https://arxiv.org/pdf/nucl-th/0004055.pdf.

[4] L. Frankfurt, et al., Coherent photo- and lepto-production of vector mesons from deuterium, Nucl. Phys. A 622 (4) (1997) 511–537, http://www.sciencedirect.com/science/article/pii/S0375947497806975.

[5] T. Mibe, et al., Measurement of coherent ϕ-meson photoproduction from the deuteron at low energies, Phys. Rev. C 76 (2007) 052202, https://doi.org/10.1103/PhysRevC.76.052202.

[6] W.C. Chang, et al., Forward coherent phi-meson photoproduction from deuterons near threshold, Phys. Lett. B 658 (2008) 209–215, https://doi.org/10.1016/j.physletb.2007.11.009, arXiv:nucl-ex/0703034.

[7] D.J. Wilson, R.A. Briceño, J.J. Dudek, R.G. Edwards, C.E. Thomas, Coupled $\pi\pi$, $k\overline{K}$ scattering in p-wave and the ρ resonance from lattice QCD, Phys. Rev. D 92 (2015) 094502, https://doi.org/10.1103/PhysRevD.92.094502.

[8] Y. Eisenberg, B. Haber, E. Kogan, U. Karshon, E. Ronat, A. Shapira, G. Yekutieli, Vector meson production by 4.3 GeV polarized photons on deuterium, Nucl. Phys. B 104 (1) (1976) 61–97, https://doi.org/10.1016/0550-3213(76)90073-0.

[9] R.L. Anderson, et al., Determination of the ρ-meson–nucleon cross section from elastic ρ photoproduction on deuterium, Phys. Rev. D 4 (1971) 3245–3250, https://doi.org/10.1103/PhysRevD.4.3245.

[10] B. Mecking, et al., The {CEBAF} large acceptance spectrometer (CLAS), Nucl. Instrum. Methods A 503 (3) (2003) 513–553, https://doi.org/10.1016/S0168-9002(03)01001-5.

[11] D. Sober, et al., The bremsstrahlung tagged photon beam in hall b at JLab, Nucl. Instrum. Methods A 440 (2) (2000) 263–284, https://doi.org/10.1016/S0168-9002(99)00784-6.

[12] Y. Sharabian, et al., A new highly segmented start counter for the CLAS detector, Nucl. Instrum. Methods A 556 (1) (2006) 246–258, https://doi.org/10.1016/j.nima.2005.10.031.

[13] E. Smith, et al., The time-of-flight system for CLAS, Nucl. Instrum. Methods Phys. Res., Sect. A, Accel. Spectrom. Detect. Assoc. Equip. 432 (2) (1999) 265–298, https://doi.org/10.1016/S0168-9002(99)00484-2.

[14] N. Compton, et al., Measurement of the differential and total cross sections of the $\gamma d \to K^0\Lambda(p)$ reaction within the resonance region, Phys. Rev. C 96 (2017) 065201, https://doi.org/10.1103/PhysRevC.96.065201.

[15] S. Stepanyan, et al., Energy calibration of the hall b bremsstrahlung tagging system using a magnetic pair spectrometer, CLAS-Note 012, https://misportal.jlab.org/ul/Physics/Hall-B/clas/viewFile.cfm/2005-012.pdf?documentId=179.

[16] E. Pasyuk, Energy loss corrections for charged particles in CLAS, CLAS-Note 016, https://misportal.jlab.org/ul/physics/hall-b/clas/viewFile.cfm/2007-016.pdf?documentId=423.

[17] T. Chetry, K. Hicks, Coherent ω-meson photoproduction off the deuteron, CLAS-Note 103, https://misportal.jlab.org/ul/Physics/Hall-B/clas/viewFile.cfm/2017-006.pdf?documentId=778.

[18] C. Patrignani, et al., Review of particle physics, Chin. Phys. C 40 (10) (2016) 100001, https://doi.org/10.1088/1674-1137/40/10/100001.

[19] F. Dietz, et al., Photoproduction of ω mesons off protons and neutrons, Eur. Phys. J. A 51 (1) (2015) 6, https://doi.org/10.1140/epja/i2015-15006-3.

[20] M. Battaglieri, et al., Photoproduction of the ω meson on the proton at large momentum transfer, Phys. Rev. Lett. 90 (2003) 022002, https://doi.org/10.1103/PhysRevLett.90.022002.

[21] M. Sargsian, 2017, private communication.